

# Spatially Resolved Joint Spectral Gamut Mapping and Separation

Sepideh Samadzadegan and Philipp Urban;  
Institute of Printing Science and Technology, Technische Universität Darmstadt;  
Magdalenenstr. 2, 64289 Darmstadt, Germany

## Abstract

The paramer mismatch-based spectral gamut mapping framework is an approach which optimizes the spectral reproduction colorimetrically for multiple viewing conditions. Unfortunately, due to the pixelwise nature of this method, almost similar neighboring pixels might be mapped to completely different colorants which yield disturbing banding artifacts. The previous proposed solution for this problem adds some noise to the  $a^*$  and  $b^*$  channels of the input images prior to calculating the separation image. Even though this procedure solves the problem of banding artifacts, it adversely affects the graininess of the final print. In this paper, we propose an approach based on both colorimetric and spatial criteria to reduce banding artifacts of the final print. To our knowledge, the proposed method is the first attempt of joint spatio-spectral gamut mapping and separation. It leads to smoother spectral separations by preserving image edges but is still not completely free of artifacts.

## Introduction

Reproduction quality may drastically be reduced by limitations of the printing system particularly by the colorimetric gamut, which is the set of printable colors for specified viewing conditions (observer, illuminant). Out of gamut colors must be mapped to in-gamut colors by gamut mapping algorithms [1] commonly with the aim of minimizing the perceived difference between the original image and the final print. To expand the printer gamut additional inks are added to the conventional CMYK ink set. Many multi-channel printers are available today utilizing, for instance, CMYKRGB inks. A byproduct of using more inks is a higher colorimetric redundancy which means that multiple colorant combinations may result in the same or almost the same color for the specified viewing condition. Corresponding reflectances are called metamers or paramers.

This colorimetric redundancy might be utilized to improve the reproduction for more than the specified viewing condition. We call such reproductions *spectral reproductions* even though perfect spectral matches between original and reproduction are rather unlikely because of the limited spectral gamut of real printing systems.

The typical spectral reproduction workflow consists of spectral gamut mapping, spectral separation, ink limitation and halftoning. In this paper we, focus on the first two stages of the workflow, i.e. spectral gamut mapping and separation. More information on ink limitation or halftoning can be found in Ref. [2, 3].

Spectral separation refers to the computation of colorant combinations for reproducing given in-gamut reflectances. This requires the inversion of a high-dimensional spectral printer model by solving a constrained optimization problem [4, 5]. Since it is rather un-

likely that an arbitrary spectral reflectance is within the spectral device gamut, spectral gamut mapping must ensure valid inputs for the separation method. Such algorithms are much more complex than conventional gamut mapping methods mainly because they have to operate within higher dimensional spaces that do not contain distance measures that correlate well with human perception. Different approaches have been proposed for specifying and accessing colorimetric gamut boundaries [6, 7]. Accessing spectral gamut boundaries is much more challenging since they are only implicitly given by the spectral printer model. For the purpose of simplifying the characterization of spectral gamut boundaries usually some kind of dimension reduction is used.

For instance, Bakke *et al.* [8] applied Principal Component Analysis (PCA) on multi-dimensional spectral data. They used the convex hull to specify the boundary of the spectral gamut. Spectral gamut mapping was performed by transforming each out-of-gamut spectra along a line towards the gamut center.

Another approach was presented by Rosen and Derhak [9]. They introduced LabPQR, a colorimetric-spectral hybrid Interim Connection Space (ICS). This space consists of three colorimetric and three spectral dimensions. The latter three dimensions are defined by the first three principal components determined by PCA on the metameric black space. The colorimetric gamut can be specified within the first three dimensions of LabPQR as used for metameric reproductions. For each CIELAB value in the colorimetric gamut, a nested gamut represented by the PQR components reflects the metameric redundancy of the printing system for this particular CIELAB color. Spectral gamut mapping is performed in this hybrid space in two stages: colorimetric and spectral. Each reflectance is converted to LabPQR. In the colorimetric stage, a traditional colorimetric gamut mapping is performed. For the resulting in-gamut color the corresponding PQR nested gamut is calculated. In the spectral stage, a PQR gamut mapping is done for PQR values outside of the nested gamut. Experiments show that spectral gamut mapping minimizing PQR differences results in minimal spectral error. However, this gamut mapping cannot guarantee minimal colorimetric errors under another than the specified viewing condition.

While the above mentioned work considers the colorimetric and spectral stages separately, there is a related spectral gamut mapping method proposed by Tsutsumi *et al.* [10] where these two stages are combined together as a single objective function. In this approach a final colorant combination is chosen by minimizing a weighted sum of normalized Euclidian distances in the PQR space and CIEDE2000 colorimetric differences in CIELAB. Due to the low-dimensionality of the ICS, spectral gamut mapping can be combined with spectral separation and encoded by smooth lookup

tables ensuring an artifact-free reproduction.

Another approach presented by Urban *et al.* [11] considers a hierarchical set of application-dependent illuminants sorted from the most to the least important one. In this approach, the CIELAB image, rendered for the first and most important illuminant, is mapped to the colorimetric gamut of the printer utilizing traditional gamut mapping methods. Also spatial gamut mapping algorithms may be used in this step (see e.g. [12]). The remaining CIELAB images, rendered for the other illuminants, are mapped to the device- and pixel-dependent metamer mismatch gamuts. These transformations use distance measures (e.g. color-difference formulas) that correlate much better with human color vision than spectral metrics. A related approach proposed by Urban and Berns [13] uses the human color quantization for exploiting spectral variability to increase colorimetric accuracy. The main idea is to map the rendered images for the second and subsequent illuminants to the device- and pixel-dependent paramer mismatch gamuts instead of metamer mismatch gamuts. This replacement utilizes the color quantization of the human visual system, i.e. colors are indistinguishable if their distance is smaller than the Just-Noticeable-Distance (JND). Considering this property of the human visual system increases the spectral variability for the second and subsequent hierarchical mappings and improves the reproduction under more illuminants.

Employing low-dimensional ICS (e.g. LabPQR) to construct lookup tables and direct computation using metamer or paramer mismatch-based frameworks can be considered as the two main noticeable approaches for spectral gamut mapping. Derhak *et al.* [14] compared the LabPQR with the metamer-mismatch framework. Their results show that LabPQR achieves a better spatial image quality but the metamer mismatch-based approach shows slightly smaller error rates.

One shortcoming of the metamer or paramer mismatch-based spectral gamut mapping is the pixelwise computation that may yield severe spatial artifacts (banding). In this paper, we combine paramer mismatch-based spectral gamut mapping with spectral separation in order to reduce such banding artifacts.

## Methodology

Although the paramer mismatch-based spectral gamut mapping framework proved to be practicable in spectral reproduction, there are some drawbacks associated with this method. Due to its pixelwise nature, similar neighboring pixels might be mapped to completely different colorant combinations yielding banding artifacts in the final reproduction (see Figure 1, second row). To avoid such artifacts Urban and Berns [13] added some noise to the  $a^*$  and  $b^*$  channel of the input CIELAB images prior to the computation of the separation image. This approach solves the problem of banding artifacts but adversely affects the graininess of the final print (see Figure 1, third row).

In order to remove banding artifacts while avoiding larger graininess of the final print, we must ensure that correlations between neighboring pixels of the final separation image agree with the correlation of corresponding pixels within the input images. For this purpose, we propose a new approach that combines spectral

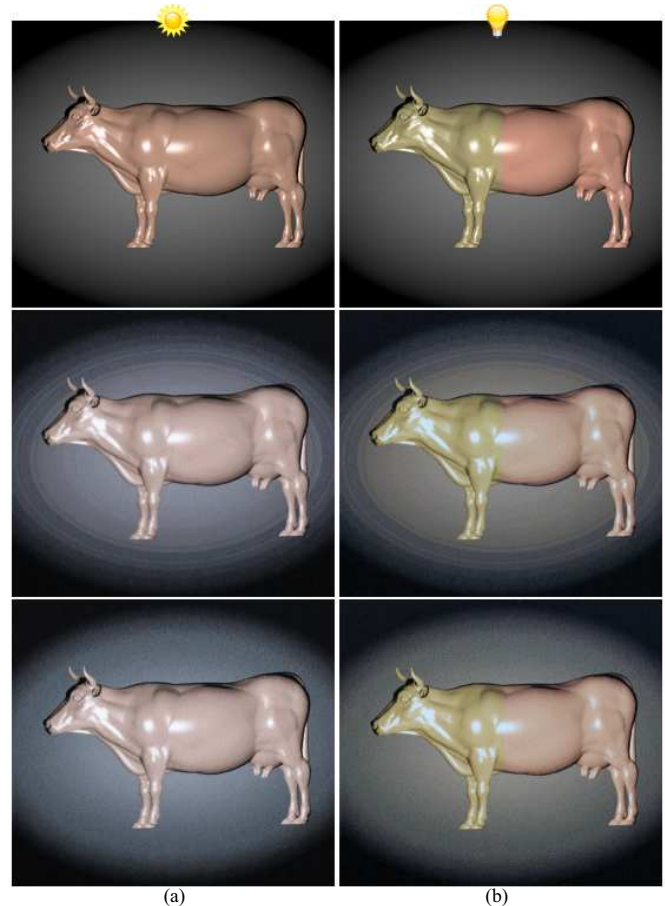


**Figure 1.** Cutout of the METACOW image [15] rendered for illuminant (a) CIED65 and (b) CIEA. First Row: original image. Second Row: Capture of a real print resulting from a pixelwise paramer mismatch-based spectral gamut mapping computation. Third Row: Capture of a real print resulting from a pixelwise paramer mismatch-based spectral gamut mapping computation after adding noise to the  $a^*$  and  $b^*$  channels of the input images. See [13].

gamut mapping and separation.

## Combining Spectral Gamut Mapping and Separation

Let  $\mathbf{R}$  be the spectral image to be reproduced and  $\mathbf{I}_1, \dots, \mathbf{I}_N$  are illuminants sorted with respect to their importance within the underlying application. For example, CIED50 can be chosen for the first illuminant  $\mathbf{I}_1$  to achieve ICC-compatible reproductions.

In a first step, the spectral image  $\mathbf{R}$  is rendered into a CIELAB image for each of the considered illuminants and specified observer. The first image (corresponding to the most important illuminant  $\mathbf{I}_1$ ) is mapped into the colorimetric gamut of the device by a conventional gamut mapping method. The resulting CIELAB images are denoted by  $\mathbf{L}_1, \dots, \mathbf{L}_N$  and are the inputs of our method.

The separation image  $\mathbf{S}$  is computed from the top-left pixel to the bottom-right pixel by a row-wise processing shown in Figure 2. For the pixel that is actually processed we consider also the

pre-processed surrounding direct neighbors. Hence, we consider  $M = 5$  pixels for computing a colorant combination that is stored at the actual pixel position in the separation image.  $M$  may be smaller for border pixels which does not affect the procedure described below. The actual pixel position is denoted by  $p_0$  and the considered neighbor pixel positions by  $p_1, \dots, p_{M-1}$ .

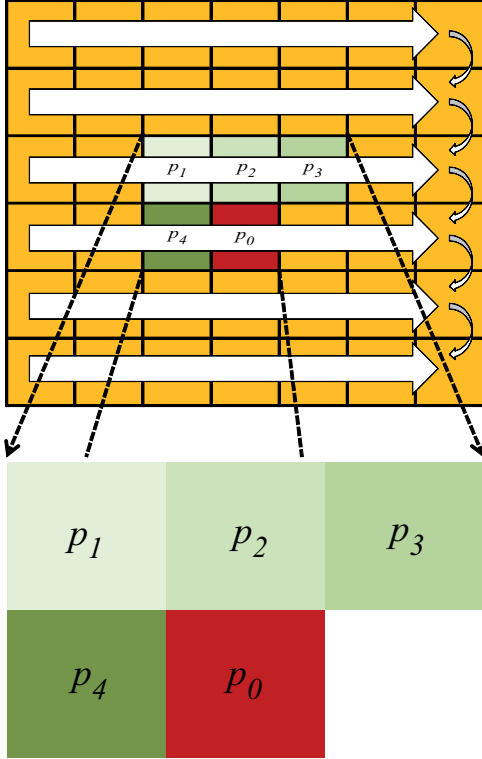


**Figure 2.** Non-iterative processing scheme: The separation image is computed by traversing from the top-left to the bottom-right pixel. For each pixel position  $p_0$ , a colorant combination is determined by minimizing a cost function that considers pre-processed surrounding neighbors  $p_1, \dots, p_4$ .

For computing the colorant combination of the separation at pixel position  $p_0$ , we solve the following optimization problem

$$\mathbf{S}(p_0) = \underset{\mathbf{x} \in \mathcal{P}(p_0)}{\operatorname{argmin}} F_{\text{cost}}(\mathbf{x}) \quad (1)$$

where  $F_{\text{cost}}$  is a cost function described below and  $\mathcal{P}(p_0)$  is the set of parametric (pixel and device dependent) colorant combinations for the first illuminant. This parametric set is defined as follows

$$\mathcal{P}(p_0) = \{ \mathbf{x} \in \Omega \mid \Delta E[\mathbf{P}_1(\mathbf{x}), \mathbf{L}_1(p_0)] \leq D \} \quad (2)$$

where  $\Omega$  is the set of all colorant combinations printable by the printer,  $\Delta E$  is a color-difference formula (e.g. CIEDE2000),  $\mathbf{P}_1(\mathbf{x})$  is the spectral printer model prediction for colorant combination  $\mathbf{x}$  rendered for the first illuminant  $\mathbf{I}_1$ ,  $\mathbf{L}_1(p_0)$  is the value at pixel position  $p_0$  of the input CIELAB image  $\mathbf{L}_1$  and  $D$  is a fraction of the JND. Note that any colorant combination within  $\mathcal{P}(p_0)$  reproduces the given CIELAB value  $\mathbf{L}_1(p_0)$  without any noticeable deviation.

## The Cost Function

The cost function is composed of a colorimetric and a spatial part

$$F_{\text{cost}}(\mathbf{x}) = 1 - F_{\text{col}}(\mathbf{x})F_{\text{spatial}}(\mathbf{x}) \quad (3)$$

where  $\mathbf{x}$  is a colorant combination,  $F_{\text{col}}(\mathbf{x})$  is the colorimetric, and  $F_{\text{spatial}}(\mathbf{x})$  is the spatial function.

The colorimetric function is defined as follows

$$F_{\text{col}}(\mathbf{x}) = \prod_{i=2}^N \exp\left(-\frac{1}{\sigma_1} \Delta E[\mathbf{P}_i(\mathbf{x}), \mathbf{L}_i(p_0)]\right) \quad (4)$$

where  $\mathbf{P}_i(\mathbf{x})$  is the spectral printer model prediction of colorant combination  $\mathbf{x}$  rendered for illuminant  $\mathbf{I}_i$ ,  $\mathbf{L}_i(p_0)$  is the CIELAB value at pixel position  $p_0$  of the original CIELAB input image rendered for illuminant  $\mathbf{I}_i$ , and  $\Delta E$  is a color-difference formula (e.g. CIEDE2000). The value  $\sigma_1 > 0$  is a weighting parameter. In the case the given pixel reflectance  $\mathbf{R}(p_0)$  is within the spectral gamut, the following equation applies  $\mathbf{P}_i(\mathbf{x}) = \mathbf{L}_i(p_0)$ ,  $i = 2, \dots, N$  and the colorimetric function is equal to one. For color differences larger than zero, the function becomes smaller than one but remains still positive. Please note that  $F_{\text{col}}$  does not depend on the pixel neighborhood.

In contrast, the spatial function  $F_{\text{spatial}}$  depends on the pre-processed neighboring pixels of the separation image  $\mathbf{S}$  at pixel positions  $p_1, \dots, p_{M-1}$ .

$$F_{\text{spatial}}(\mathbf{x}) = \exp\left(-\frac{1}{\sigma_2} \left\| \sum_{j=1}^{M-1} \omega(p_j) \mathbf{S}(p_j) - (1 - \omega(p_0)) \mathbf{x} \right\|_2\right) \quad (5)$$

where the value  $\sigma_2 > 0$  is a weighting parameter,  $\mathbf{S}(p_j)$ ,  $j = 1, \dots, M-1$ , are pre-processed colorant combinations of neighboring pixels, and  $\omega(p_j) \geq 0$ ,  $j = 0, \dots, M-1$  are weights satisfying  $\sum_j \omega(p_j) = 1$ . These weights specify the contribution of each of the considered colorant combinations. The term within the 2-norm is the difference between  $\mathbf{x}$  and a weighted average of colorant combinations (including  $\mathbf{x}$  and  $\mathbf{S}(p_j)$ ,  $j = 1, \dots, M-1$ ). In smooth image areas of the input CIELAB images the weights must be selected to be similar. In this case, the weighted average is also similar to an un-weighted average, i.e. if  $\mathbf{x}$  is similar to the considered pre-processed colorant combinations the 2-norm difference becomes small.

In the case the input CIELAB images contain sharp edges, the contribution of colorant combinations lying on the other side of the edge (with respect to the actual pixel position) must be small. In this situation, colorant combinations  $\mathbf{x}$  very different to the colorant combinations on the other side of the edge result in small 2-norm differences as well. In summary, we need weights which ensure an edge preserving smooth separation image.

The main idea for computing the weights,  $\omega(p_j) \geq 0$ ,  $j = 0, \dots, M-1$ , is adopted from bilateral filtering used for edge-preserving image smoothing [16]. Instead of employing spatial distance and range differences for computing the weights, we apply color-differences across illuminants. Our weight function employed in eq. (5) is defined as follows

$$\omega(p) = \frac{\prod_{i=1}^N \exp\left(-\frac{1}{\delta} \Delta E [\mathbf{L}_i(p_0), \mathbf{L}_i(p)]\right)}{\sum_{j=0}^{M-1} \prod_{i=1}^N \exp\left(-\frac{1}{\delta} \Delta E [\mathbf{L}_i(p_0), \mathbf{L}_i(p_j)]\right)} \quad (6)$$

where all variables are denoted as before and  $\delta > 0$  is a weighting parameter. The denominator ensures that the weights sum up to one. Positive parameters  $\sigma_1$  and  $\sigma_2$  are used (see eq. (4) and eq. (5)) to balance the contribution of  $F_{\text{col}}$  and  $F_{\text{spatial}}$ .

## Results and Discussion

In the present work, we are not interested in any colorimetric or spectral accuracy, which would only reflect the accuracy of the spectral printer model. Furthermore, the separation shall not depend on the halftoning algorithm. Banding artifacts are already apparent within the separation image when edges are introduced in spatially homogeneous areas of the input image. Therefore, we investigate resulting separation images and compare them with images computed by the pixelwise paramer-mismatch based spectral gamut mapping approach [13].

For our experiments, we used an HP Designjet Z3100 printer and the Onyx ProductionHouse RIP. We employ only the CMYKRGB standard ink set. The printer was characterized as a combination of 20 four-ink cellular Yule-Nielsen modified Neugebauer (CYNSN) models [17, 18, 19, 20] as used by Urban and Berns [13] and proposed by Tzeng and Berns [4]. For computing the parameric sets (see eq. (2)) we divided the hue-linear nearly perceptually-uniform LAB2000HL color space [21] into cubes with a side length of approx. 0.4 CIEDE2000. This side length is below the JND for standard office viewing conditions. We sampled the colorant space of each of the 20 printer models in steps of approx. 1% resulting in nearly  $10^8$  colorant combinations. These colorant combinations were transformed into LAB2000HL for illuminant  $\mathbf{I}_1$  by each printer model. All colorant combinations whose printer model LAB2000HL predictions fall into a cube were stored in a separate list allowing a quick access to the corresponding parameric colorant set. Variables required to compute the cost function  $F_{\text{cost}}$  are directly extracted from the list and from the input CIELAB images. We parametrized our cost function using  $\sigma_1 = 3$ ,  $\sigma_2 = 20$ , and  $\delta = 2$ . These values were adjusted based on visual inspection of resulting separations which may leave room for improvement. In future work, image quality measures shall be used as objective functions to optimize parameter fitting.

For our experiment we used the METACOW image designed by Fairchild and Johnson [15]. This image is a spectral target consisting of 24 cows arranged similarly as the patches in a color checker target. The rear and front of each cow are metamers under CIED65 with a particularly large color difference under CIEA. To illustrate the advantages and shortcomings of the proposed method, it is sufficient to choose only a cutout of the METACOW image. We used the cow shown in Figure 1 (top row).

Figure 3 shows the separation bands for the black and for the red ink. The other bands are omitted for the sake of brevity and because they do not give more information. Compared to the pixelwise approach, the spatial method shows much smoother

transitions. This is particularly apparent in the background. Nevertheless, there is still some room for improvement, since not all stripes could be avoided. Edges are preserved by the spatial approach. Please note that also the *metameric edge* between the rear and the front part of the cow is preserved.

In order to compare the reproduction accuracy of the pixelwise paramer-mismatch based spectral gamut mapping approach with its spatial extension, we use  $\Delta E_{ab}^*$  color differences for the considered illuminants. Note that spectral differences (e.g. RMS errors) are not used as objective functions in neither of the approaches and give almost no information on the color errors under the considered illuminants.

We are particularly interested in how the described spatial modifications impair colorimetric results. For this, we apply the forward printer model to both separations (based only on colorimetric criteria and based upon colorimetric and spatial criteria) and computed color differences between the resulting reproductions and the original image. Since the colorimetric gamut mapping strategy is similar for both approaches, we present the gains of color deviations resulting from the spatial modification. These gains are not biased by any errors resulting from out-of-gamut colors. The table depicts the maximum and average gains of the  $\Delta E_{ab}^*$  color differences for the investigated cutout of the METACOW image. At least for this example, the gain of colorimetric errors is negligible.

	CIED65	CIEA
max	1.0185	1.0185
avg	0.1193	0.1899

### $\Delta E_{ab}^*$ color error gains between the colorimetric and the spatially-enhanced separation.

The required running time for computing and storing the nearly  $10^8$  colorant combinations is approximately 15.2 minutes on an *Intel(R)Core(TM)i7 - 3820CPU@3.60GHz* processor. This computation is required only once after calibrating and characterizing the printing system. Extracting the control values for the separation utilizing only the colorimetric part of the cost function, takes about 10.7 minutes for the one mega-pixel METACOW image on the same hardware. Considering the spatial extension, the time gain is roughly 1.8 minutes. Note that particularly the separation-pooling is performed by a not performance-optimized single-threaded code. This leaves much room for decreasing the running time of the computation.

A shortcoming of the presented method is a smearing effect apparent on the right side of edges particularly to the right of the cow. This might result in artifacts within the final print. We assume that spatial separation errors are propagated and accumulated causing this effect. Distributing such errors over a large spatial area might reduce their visibility, similarly as in error diffusion halftoning. This shall be addressed in future research.

## Conclusions

In this paper, an approach for joint spectral gamut mapping and separation was proposed that reduces banding artifacts in spectral prints. The method adapts the paramer mismatch-based spec-

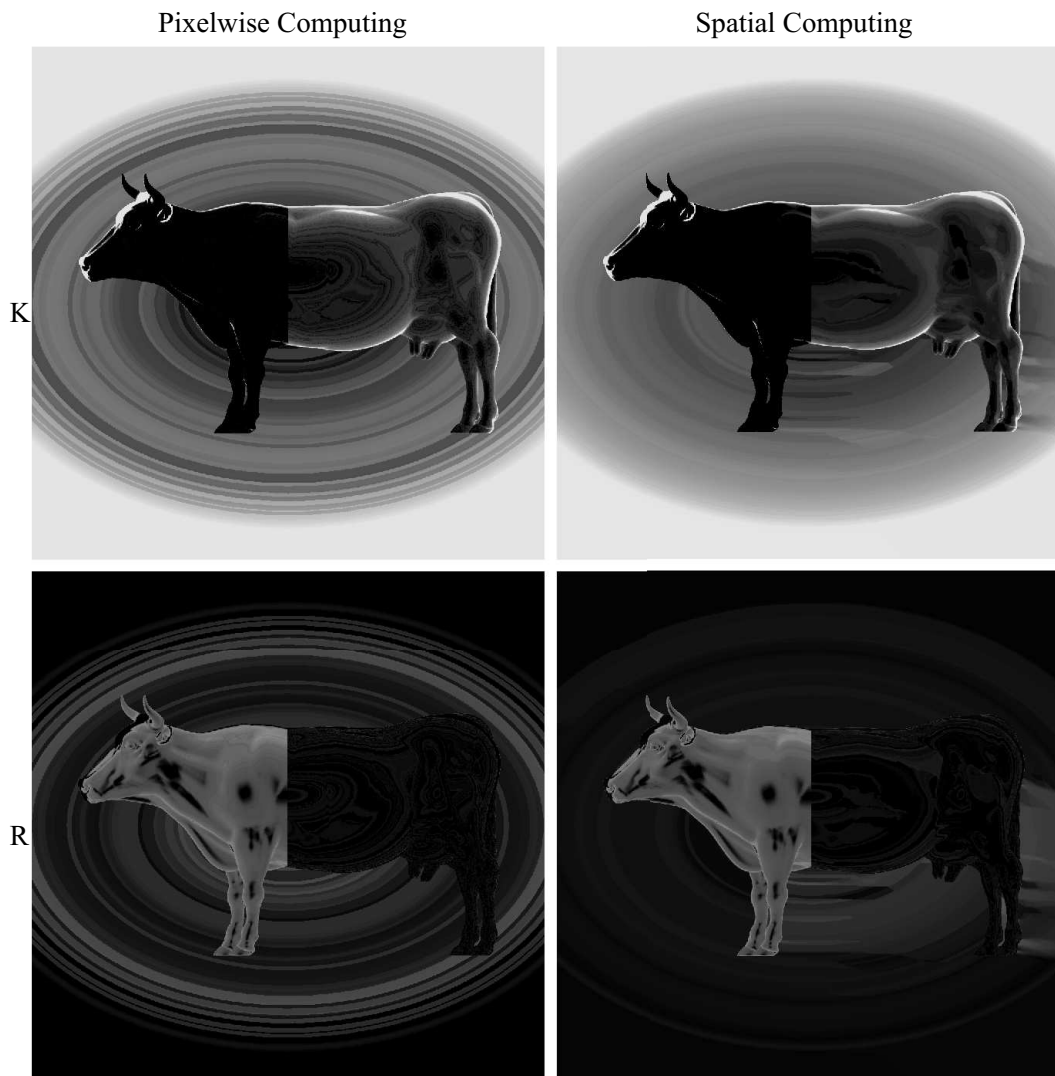


**Figure 3.** Separation bands of the black (K) and red (R) ink computed by the pixelwise (left) and the spatial (right) approach.

tral gamut mapping framework and considers spatial information to smooth the separation by preserving edges. For this purpose, a cost function was introduced which considers colorimetric criteria as well as local spatial correlations of the input image. The separation is computed by traversing the image from the top-left to the bottom-right pixel and selecting a colorant combination for each pixel which minimizes the cost function. To our knowledge, this is the first attempt of joint spatio-spectral gamut mapping and separation. An experiment illustrated that the method results in smoother separations compared to a pixelwise approach. Smearing artifacts suggest to distribute processing errors over a large image area to minimize their visibility.

### Acknowledgements

This work was supported by the Marie Curie Initial Training Networks (ITN) CP7.0 N-290154 funding, which is gratefully acknowledged.

### References

- [1] J. Morovič. *Color Gamut Mapping*. John Wiley & Sons, 2008.
- [2] P. Urban. Ink Limitation for Spectral or Color Constant Printing. In *11th Congress of the International Colour Association*, Sydney, Australia, 2009.
- [3] D.L. Lau and G.R. Arce. *Modern Digital Halftoning*. 3 edition.
- [4] D.-Y. Tzeng and R. S. Berns. Spectral-Based Six-Color Separation Minimizing Metamerism. In *IS&T/SID*, pages 342–347, Scottsdale Ariz., 2000.
- [5] P. Urban, M. R. Rosen, and R. S. Berns. Fast Spectral-Based Separation of Multispectral Images. In *IS&T/SID, 15th Color Imaging Conference*, pages 178–183, Albuquerque, New Mexico, 2007.
- [6] M. Mahy. Gamut calculation of color reproduction devices. In *IS&T/SID*, pages 145–150, Scottsdale Ariz., 1995.
- [7] J. Morovic and M. R. Luo. Calculating medium and image gamut boundaries for gamut mapping. *Color Research and*

*Application*, 25:394–401, 2000.

- [8] A. M. Bakke, I. Farup, and J. Y. Hardeberg. Multispectral Gamut Mapping and Visualization - A First Attempt. volume 5667, pages 193–200. SPIE, 2005.
- [9] M.R. Rosen and M.W. Derhak. Spectral Gamuts and Spectral Gamut Mapping. In *Spectral Imaging: Eighth International Symposium on Multispectral Color Science*, San Jose, CA, 2006. SPIE.
- [10] S. Tsutsumi, M. R. Rosen, and R. S. Berns. Spectral Gamut Mapping using LabPQR. *Journal of Imaging Science and Technology*, 51(6):473–485, 2007.
- [11] P. Urban, M. R. Rosen, and R. S. Berns. Spectral Gamut Mapping Framework Based on Human Color Vision. In *CGIV*, pages 548–553, Barcelona, Spain, 2008.
- [12] P. Zolliker and K. Simon. Retaining local image information in gamut mapping algorithms. *IEEE Transactions on Image Processing*, 16(3):664–672, 2007.
- [13] P. Urban and R. S. Berns. Paramer Mismatch-based Spectral Gamut Mapping. *IEEE Transactions on Image Processing*, 20(6):1599–1610, 2011.
- [14] M.W. Derhak and R.S. Berns. Comparing LabPQR and the spectral gamut mapping framework. In *IS&T/SID, 18th Color Imaging Conference*, pages 206–212, San Antonio, Texas, 2010.
- [15] M. D. Fairchild and G. M. Johnson. METACOW: A Public-Domain, High-Resolution, Fully-Digital, Noise-Free, Metameric, Extended-Dynamic-Range, Spectral Test Target for Imaging System Analysis and Simulation. In *IS&T/SID, 12th Color Imaging Conference*, pages 239–245, Scottsdale Ariz., 2004.
- [16] C. Tomasi and R. Manduchi. Bilateral Filtering for Gray and Color Images. In *Computer Vision, 1998. Sixth International Conference on*, pages 839–846, 1998.
- [17] J. A. C. Yule and W. J. Nielsen. The penetration of light into paper and its effect on halftone reproduction. In *Tech. Assn. Graphic Arts*, volume 4, pages 65–76, 1951.
- [18] J. A. C. Yule and R. S. Colt. Colorimetric Investigations in Multicolor Printing. In *TAGA Proceedings*, pages 77–82, 1951.
- [19] J.A.S. Viggiano. The Color of Halftone Tints. In *TAGA Proceedings*, pages 647–661, 1985.
- [20] J.A.S. Viggiano. Modeling the Color of Multi-color Halftones. In *TAGA Proceedings*, pages 44–62, 1990.
- [21] I. Lissner and P. Urban. Toward a unified color space for perception-based image processing. *Image Processing, IEEE Transactions on*, 21(3):1153–1168, 2012.

## Author Biographies

*Sepideh Samadzadegan started her research in the color research group at Technische Universität Darmstadt (Germany) since 2012 as an EU-researcher involved in the Colour Printing 7.0 | Next generation multi-channel printing (CP 7.0) project. Her research focus is on spectral gamut prediction and mapping. She is currently a technical member of the CIE TC 8-13 Colour Gamuts for Output Media. She holds a Msc in Media Technology and Engineering (Advanced Computer Graphics) from Linköping University, Norrköping Campus, Sweden.*

*Philipp Urban has been head of an Emmy-Noether research group at the Technische Universität Darmstadt (Germany) since*

*2009. His research focuses on color science and spectral imaging. From 2006–2008 he was a visiting scientist at the RIT Munsell Color Science Laboratory. He holds a MS in mathematics from the University of Hamburg and a PhD from the Hamburg University of Technology (Germany).*